PHYSICO-CHEMICAL BASICS OF METALLURGICAL PROCESSES / ФИЗИКО-ХИМИЧЕСКИЕ ОСНОВЫ МЕТАЛЛУРГИЧЕСКИХ ПРОЦЕССОВ

UDC 669.017.15
DOI 10.17073/0368-0797-2025-1-69-75

Original article
Оригинальная статья

Construction of liquidus surface of Fe – B – Mn – C – Cr five-component diagram

G. A. Kazakevich ✉, **A. Yu. Popov**

Russian University of Transport (9, bld. 9 Obraztsova Str., Moscow 127994, Russian Federation)

✉ KazakevichG@mail.ru

Abstract. The authors used the technique of constructing the schemes of multicomponent diagrams ($n > 3$) in traditional coordinates "temperature – concentration", the basis of which are n – angles with a divergent coordinate grid at $n > 4$, to construct the liquidus surface of the Fe–B–Mn–C–Cr five-component system. Choice of the system was determined by the need to harden the surfaces of parts made from a large number of low-alloy steels by boriding. The critical points of the liquidus surface were melting points of the alloy chemical elements, melting points of borides and melting temperatures of eutectics of the phase diagrams, which are the sides of a pentahedral prism. Individual experimental melting temperatures of the steels and calculated melting temperatures of new eutectics during the interaction of eutectics of double phase diagrams were also taken into account. The latter were determined according to the eutectic reaction rule, which provides for the use of only melting temperatures of the initial eutectics in the calculation. At the same time, phase composition of the multicomponent boride eutectics of the system was determined. The resulting liquidus surface shows the temperature at which crystallization begins and the phase composition of the layer during boriding of casting mold coatings for surface hardening of castings. The calculated melting temperatures of eutectics form the solidus surfaces of the system. In accordance with the concentration values of the elements, especially boron, five solidus surfaces are formed in the system at 1571, 1451, 1394, 1105 and 978 °C. These melting temperatures of eutectics are the boundaries between the diffusion and diffusion-crystallization mechanisms of formation of boronized layer in solid and solidifying states of treated surfaces, therefore, they determine the mechanism of formation of boronized layer, their phase composition, structural morphology and properties.

Keywords: liquidus surface, five-component system, calculation of eutectic temperatures, divergent grid, phase diagram, steel, boriding

For citation: Kazakevich G.A., Popov A.Yu. Construction of liquidus surface of Fe–B–Mn–C–Cr five-component diagram. *Izvestiya. Ferrous Metallurgy*. 2025;68(1):69–75. https://doi.org/10.17073/0368-0797-2025-1-69-75

Построение поверхности ликвидус пятикомпонентной схемы диаграммы Fe – B – Mn – C – Cr

Г. А. Казакевич ✉, **А. Ю. Попов**

Российский университет транспорта (Москва, 127994, ул. Образцова, 9, стр. 9)

✉ KazakevichG@mail.ru

Аннотация. Для построения поверхности ликвидус пятикомпонентной системы Fe–B–Mn–C–Cr применялась методика построения в традиционных координатах «температура – концентрация» схем многокомпонентных диаграмм ($n > 3$), основанием которых являются n-угольники с дивергентной координатной сеткой при $n > 4$. Выбор системы обусловлен необходимостью упрочнения поверхностей деталей, изготовленных из большого количества низколегированных сталей борированием. Критическими точками поверхности ликвидус являлись температуры плавления химических элементов сплава, боридов и эвтектик двойных диаграмм состояния, которые являются сторонами пятигранной призмы. Принимались во внимание также отдельные экспериментальные температуры плавления сталей и рассчитанные температуры плавления новых эвтектик, образующихся при взаимодействии эвтектик двойных диаграмм состояния. Последние определялись по правилу эвтектической реакции, предусматривающему использование при расчете только температур плавления исходных эвтектик. Одновременно определялся и фазовый состав многокомпонентных боридных эвтектик системы. Полученная поверхность ликвидус показывает температуру начала кристаллизации и фазовый состав слоя при проведении борирования из обмазок литейных форм для поверхностного упрочнения отливок. Рассчитанные температуры плавления эвтектик образуют поверхности солидус системы. В соответствии с концентрационными значениями элементов, и особенно бора, в системе образуются пять поверхностей солидус при 1571, 1451, 1394, 1105 и 978 °C. Данные температуры плавления эвтектик являются границами между диффузионным и диффузионно-кристаллизационным механизмами формирования борированных слоев в твердом и затвердевающем

состояниях обрабатываемых поверхностей. Следовательно, они определяют механизм формирования борированных слоев, их фазовый состав, структурную морфологию и свойства.

Ключевые слова: поверхность ликвидус, пятикомпонентная система, расчет эвтектических температур, дивергентная сетка, диаграммы состояния, стали, борирование

Для цитирования: Казакевич Г.А., Попов А.Ю. Построение поверхности ликвидус пятикомпонентной схемы диаграммы Fe–B–Mn–C–Cr. *Известия вузов. Черная металлургия*. 2025;68(1):69–75. https://doi.org/10.17073/0368-0797-2025-1-69-75

Introduction

Phase diagrams of alloys serve as essential reference tools for both theorists and practitioners in metallurgy, materials science, metal forming, casting, various fields of mechanical engineering, and the operation of technical equipment.

Taking into account that most of the steels and alloys used are multicomponent ($n > 3$), in many cases certain difficulties arise in determining the conditions for performing technological processes, the phase composition and properties of alloys, since there are no constructed state diagrams in the temperature-concentration traditional coordinates [1 – 3]. Typically, binary and ternary diagrams, their isothermal sections, tetrahedral representations for specific temperatures, and practical research findings are used to describe these processes [4 – 6].

In particular, binary and ternary phase diagrams have been widely applied to describe the boriding process and the properties of boronized layers [7 – 9]. These diagrams refine the concentrations of compounds and solid solutions, define phase transformation temperatures, and reveal new compounds. A key finding is the confirmed existence of iron borocarbide [8; 9], which has the formula $Fe_{23}(C, B)_6$. In other complex carbides found in steels, alloying elements typically substitute for iron.

It has been established that at 1000 °C, up to 80 % of the carbon in cementite can be replaced by boron, modifying the formula to $Fe_3C_{0.2}B_{0.8}$. This substitution alters the crystal lattice parameters, leading to compression along the a and c axes and expansion along the *b* axis of the orthorhombic lattice. Additionally, as boron content increases, the saturation magnetization and Curie temperature also rise. This phenomenon is crucial in explaining the properties of borided components, where borocarbide inclusions form beneath the boride layer [10; 11].

Study [8] demonstrated that borocarbide $Fe_{23}(C, B)_6$ is isomorphic to cubic chromium carbide $Cr_{23}C_6$ (structure type *d*84). As the composition shifts from carbon-enriched to boron-enriched, the lattice parameter *a* increases from 1.0594 to 1.0628 nm. When heated to 800 °C $Fe_{23}(C, B)_6$ melts congruently. Isothermal sections at 700, 800, 900, and 1000 °C indicate that the $Fe_{23}(C, B)_6$ phase has a composition corresponding to $Fe_{23}(C_{0.73}B_{0.27})_6$ and is in equilibrium with borocementite $Fe_3(C, B)$ and Fe_α. The phase $Fe_{23}(C_{0.44}B_{0.56})_6$ is in equilibrium with Fe_2B and $Fe_3(C, B)$. An analysis of the section at 800 °C shows that $Fe_{23}(C, B)_6$ exists over a wider range of carbon and boron concentrations, between $Fe_{23}(C_{0.38}B_{0.62})_6$ and $Fe_{23}(C_{0.77}B_{0.23})_6$, and is in equilibrium with Fe_γ and $Fe_3(C, B)$. It has been determined that $Fe_{23}(C, B)_6$ remains stable up to 965 ± 5 °C [12 – 14]. These findings refine the phase composition of phase diagram regions and the properties of borided layers, as borocarbide inclusions exhibit high hardness [15 – 17].

In the study of multicomponent phase diagrams ($n > 3$), the thermodynamic method, which incorporates the characteristics of binary phase diagrams, has been widely used [18]. Specifically, a four-component Fe – Mn – Si – C phase diagram was developed by calculating thermodynamic constants at the phase transformation temperatures of compounds, followed by triangulation of the system and its subsystems. This resulted in a tetrahedral phase diagram consisting of 16 elementary tetrahedra containing congruently and incongruently melting compounds [19].

The Bukke-Schout method [20] represents the system's composition or state as a tetrad on a plane, though it is derived from a four-dimensional figure. However, the systems described in studies [21; 22] create geometric representations of multicomponent compositions in two dimensions, making them less suitable for practical applications. The refinements of the general approach discussed in studies [23; 24] do not produce practical working diagrams but instead generate planar projection systems after double projection, which are also difficult to use as working schematics in technological process development.

To determine the temperatures of eutectic reactions and the compositions of eutectic alloys, differential scanning calorimetry [25; 26], metallographic studies [27; 28], and *X*-ray diffraction analysis [29] have traditionally been used. These methods, however, are labor-intensive, leading to the increasing use of analytical and statistical approaches for predictive calculations of these characteristics.

A statistical method has been proposed for calculating eutectic temperatures and concentrations in metallic multicomponent systems ($n > 3$), where the only input data are the melting temperatures of the components forming the eutectic or the calculated eutectic melting temperatures resulting from their interaction. In this context, a temperature rule for eutectic reactions has been formulated [30; 32].

The methodology proposed in study [32], based on a developed database incorporating calculation programs and a recursive algorithm, is applicable to simple systems. However, it does not account for the formation of chemi-

cal compounds in multicomponent systems, the presence of multiple eutectics in binary systems, or the formation of solid solutions. A more advanced method that considers atomic electric charges and their interactions [33] also has these limitations, while further complicating theoretical justification and calculations.

Another approach involves calculating eutectic and peritectic temperatures and compositions in binary systems using approximation techniques to model the relationships between these characteristics. These calculations are performed using fractional-linear and power functions, relying only on the melting temperatures of the components [34], or by applying linear geometry to determine the eutectic composition of a binary system based on the known melting temperatures of its components and eutectic [35].

One method for constructing schemes of multicomponent ($n > 3$) phase diagrams in traditional *temperature – concentration* coordinates is the approach proposed in studies [36 – 38]. This method uses the *Krukovich divergent coordinate grid* to determine the distribution of alloying elements over the diagram's base area – a concentration *n*-gon, where the number of vertices corresponds to the number of chemical elements in the alloy. The sides of the polyhedral prism represent binary phase diagrams. These phase diagrams, referred to as diagram schemes, omit certain combinations of alloying elements in the concentration polyhedron. Specifically, alloys with equal proportions of three elements are absent in a four-component system, four elements in a five-component system, and so on. Nevertheless, these schemes provide a highly illustrative representation and can serve as a technological reference diagram for analyzing alloy states.

Thus, this study aims to construct the liquidus surface for the multicomponent Fe – B – Mn – C – Cr system, following the recommendations from [36 – 38] to determine saturation temperatures and explain the structural formation processes that occur during boriding in different aggregate states of treated surfaces.

Results and discussion

A wide range of steel grades and alloys, including (AISI) C1020, 5140, L6, D3, 430, SCSiMn2 (Japanese), W 1-0.8 C EXTRA, and others, undergo boriding to enhance wear resistance. Many structural steels are characterized by a combination of Fe – Mn – C – Cr elements. Components made from these steels are borided in both the solid state and the liquid state within casting molds, as well as through partial remelting of the hardened surfaces (in the presence of both liquid and solid phases) when using concentrated heat sources. In such cases, knowledge of melting temperatures involving boron is essential, leading to a system represented as Fe – Cr – Mn – C – B, where the sequence of elements is chosen arbitrarily.

The construction of the liquidus surface for the five-component Fe – B – Mn – C – Cr phase diagram, with the selected sequence of elements, was carried out by analyzing the structural formation of binary phase diagrams of alloys. This process incorporated experimental critical points of several alloys in the system, as well as calculated temperatures and concentrations of eutectic interactions. In particular, when determining boriding conditions for alloy steels and alloys, both binary and ternary phase diagrams containing iron were analyzed, along with binary diagrams that included only alloying elements and boron. To predict the type of borides and their degree of alloying, the isomorphism of boride crystal lattices and the solubility of borides within each other were considered. It can be assumed that the formation of a particular primary boride during alloy saturation with boron depends on the affinity of the elements for boron and the amount of the base element in the alloy. Therefore, in this case, the shape of the liquidus surface is determined by the concentration distribution of boron.

Fe – Cr – B system: at 1000 °C, the phases in equilibrium with γ-Fe include α-Fe and Fe_2B, while those in equilibrium with the α-phase include γ-Fe, Fe_2B, Cr_2B, and Cr_4B. The Fe_2B and, particularly, Cr_2B phases form extensive regions of solid solutions [36]. It has been established that within the boriding temperature range of 700 – 1250 °C, no ternary phases are formed in this system.

Cr – Mn – B system: at 800 °C, an unlimited series of solid solutions (Cr, Mn)B_2, (Cr, Mn)$_3B_4$, and between Cr_2B and Mn_4B borides has been identified [36]. The degree of mutual solubility of borides is as follows: Cr_5B_3 dissolves 0.08 mass fractions of Mn_5B_3 boride, while CrB dissolves 0.20 mass fractions of MnB; MnB dissolves 0.4 mass fractions of CrB.

An alternative interpretation of the binary phase diagram for the Mn – B system suggests the existence of an unlimited series of solid solutions (Cr, Mn)$_2$B instead of the Cr_2B – Mn_4B system at 1025 °C. Study [39] determined the compositions of solid solutions of chromium and manganese monoborides: $Cr_{0.46}Mn_{0.54}B$ and $Mn_{0.60}Cr_{0.40}B$. The region between the solid solutions based on CrB and MnB corresponds to the $Cr_xMn_{1-x}B$ boride.

It should also be noted that isomorphic borides of Fe and Mn (FeB and MnB, Fe_2B and Mn_2B) exhibit unlimited mutual solubility.

According to the selected technique for constructing schemes of multicomponent phase diagrams, each element of the system is distributed within the volume of the pentahedral prism from two faces and across the base area (a pentagon) from two sides. For example, carbon is distributed from the C – Cr and C – Mn sides (Fig. 1). The concentration distribution of any element across the pentagon's surface, calculated using the divergent coordinate grid, is non-uniform. The divergence angle of each coordinate line was determined by the formula

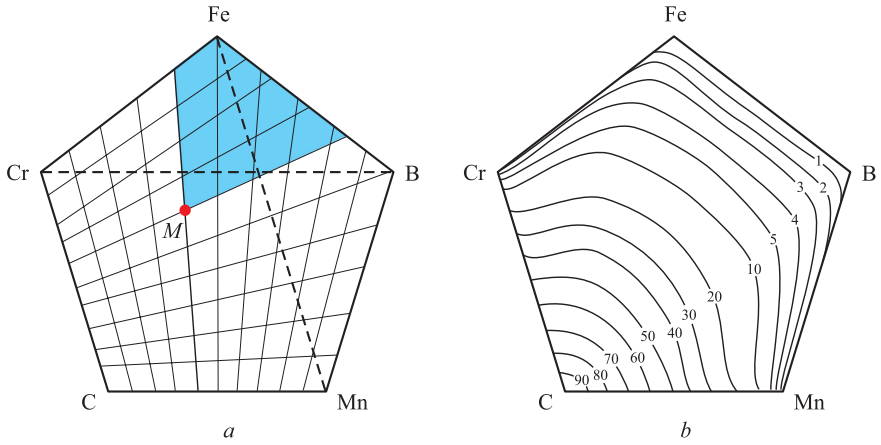

Fig. 1. Basis of the five-component phase diagram with a divergent coordinate grid (*a*) and concentration distribution of carbon in wt. % (*б*) (distribution stencil for any element)

Рис. 1. Основание схемы пятикомпонентной диаграммы состояний с дивергентной сеткой координат (*а*) и концентрационное распределение углерода, мас. % (*б*) (трафарет распределения для любого элемента)

$$\alpha = \left(1 - \frac{4}{n}\right)\frac{180}{c},$$

where n is the number of components in the system (i.e., the number of polygon sides), and c is the number of divisions on the uniform concentration scale.

In this case, the divergence angle of each coordinate line from the previous one is 3.6° for $c = 10$. The shaded area enclosed by the coordinate lines (Fig. 1) represents the carbon content at point *M*, expressed as a percentage of the pentagon's total area. This area was determined geometrically. The calculated concentrations at multiple points allowed for the construction of iso-concentration lines across the base of the pentahedral prism, collectively forming a stencil for element distribution.

To determine the concentration of another element at point *M* (e.g., boron), the stencil is rotated so that 100 % aligns with vertex B (boron). The intersection of point *M* with the corresponding iso-concentration line indicates the boron content (Fig. 2), which, in this case, is 10 wt. %.

The liquidus surface for the selected element arrangement is formed by a set of critical points, including the onset of crystallization of chemical elements and solid solutions, the melting temperatures of congruently melting phases, the melting points of binary eutectics from phase diagrams of alloys, and their interactions leading to the formation of new multicomponent eutectics. The two observed peaks correspond to the formation of alloyed chromium borides (Cr, Fe, Mn)B (~2100 °C) and (Cr, Fe, Mn)B_2 (~2200 °C) at these boron and chromium concentrations (Fig. 3).

At high boron concentrations, high-temperature eutectics from the Fe–B and Mn–B binary phase diagrams

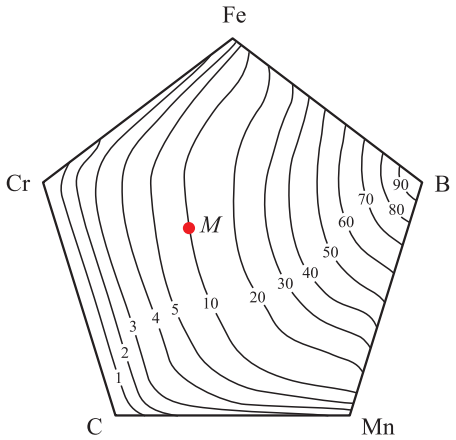

Fig. 2. Determination of boron content at point *M*

Рис. 2. Определение содержания бора в точке *M*

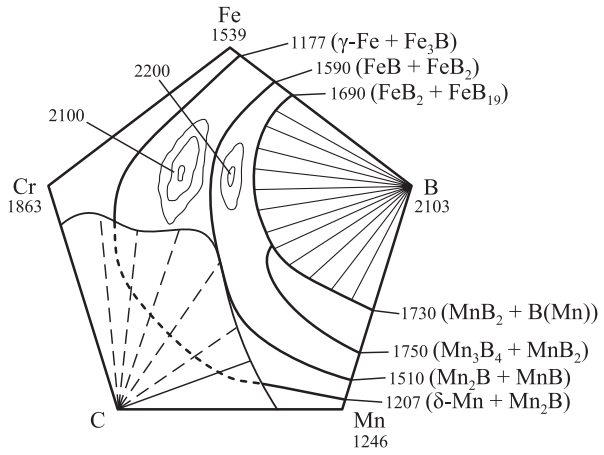

Fig. 3. Liquidus surface of the Fe–B–Mn–C–Cr system with indicated temperatures, phase composition of eutectics and lines of their interaction (top view)

Рис. 3. Поверхность ликвидус системы Fe–B–Mn–C–Cr с обозначенными температурами, фазовым составом эвтектик и линиями их взаимодействия (вид сверху)

interact, forming a new eutectic mixture $FeB_2 + FeB_{19} + Mn_3B_4 + MnB_2 + B(Mn)$ with a calculated melting temperature of 1571 °C. In the presence of a sufficient amount of chromium and a boron concentration in the range of 27.92 – 90.0 wt. %, the formation of a eutectic containing $(Fe, Mn)B_2 + FeB_{19} + Mn_3B_4 + B(CrMn) + CrB_2$ possible, with a calculated melting temperature of 1394 °C.

At boron concentrations between 16.25 and 27.92 wt. %, the interaction of $FeB + FeB_2$ and $Mn_2B + C$ eutectics results in the formation of a eutectic mixture $(Fe, Mn)B + FeB_2 + Mn_2B$ with a calculated melting temperature of 1451 °C.

At boron concentrations between 0.01 and 10 wt. %, the interaction of the γ-Fe – Fe_3B and δ-Mn + Mn_2B eutectics leads to the formation of a new eutectic mixture γ-Fe + Fe_3B + δ-Mn + Mn_2B a calculated melting temperature of 1105 °C. At chromium concentrations above 40 wt. %, another eutectic may form (γ-Fe + Fe_3B + + δ-Mn + Mn_2B) + Cr(B) + Cr_2B with a melting temperature of 978 °C. The phase compositions resulting from eutectic interactions are presented without considering the mutual solubility of borides.

The melting temperatures of congruently melting borides FeB, FeB_2, Mn_2B, Mn_3B_4, MnB, Mn_3B_4, MnB_2 and their interactions are not included in the liquidus surface visualization for clarity. The temperature of the liquidus surface is crucial for boriding castings in molds coated with a boriding mixture, as well as for predicting the phase composition of the boronized layer.

The calculated melting temperatures of new eutectics represent the lowest temperatures at which alloy melting begins, i.e., the solidus surface temperature. This temperature defines the boundary for the formation of boronized layers through a diffusion mechanism in the solid state of treated surfaces and a diffusion-crystallization mechanism in the solidifying state of surfaces.

Eutectic temperatures were calculated in accordance with Krukovich's eutectic reaction rule [17; 30; 31; 36 – 38; 40] using the following formulas:

– for an even number of eutectic components ($2n$)

$$T_{eut} = K_{eut}^{n/2} \sum_{i=1}^{n} T_i;$$

– for an odd number of eutectic components ($2n + 1$)

$$T_{eut} = K_{eut}^{\frac{n+1}{2}} \sum_{i=1}^{n-1} T_i + K_{eut} T_n;$$

$$K_{eut} = 0.497 \exp(-0.2657X);$$

$$X = \frac{\sum_{1 \le i \le j \le n}^{n} |T_i - T_j|}{\left(\sum_{i=1}^{n} T_i\right)^{0.74}},$$

where T represents the melting temperatures of eutectic phases or the melting temperatures of binary (or ternary) eutectic interactions, which form the components of a new eutectic mixture, K; K_{eut} is the eutectic temperature coefficient, and X is a temperature scaling parameter.

According to the eutectic reaction rule, when calculating the eutectic temperature of a new eutectic, the melting temperatures of binary eutectics or previously calculated eutectics (whose components also form part of the new eutectic mixture) were used.

The phase composition, structural morphology, and properties of boronized layers depend depend on the content of alloying elements in the steel, the saturation temperature, and the saturation potential of the environment. Specifically, during the boriding of 5140 steel (AISI), which contains contains 0.36 – 0.44 % C, 0.17 – 0.27 % Si, 0.5 – 0.8 % Mn, and 0.8 – 1.1 % Cr, at a saturation temperature of 950 °C in a boriding mixture ensuring a boron concentration of ~17 %, layers based on alloyed borides $(Fe, Cr)B + (Fe, Cr, Mn)_2B$ are formed. When the melting temperature is exceeded, heterogeneous layers develop, where dispersed alloyed borides are embedded in an α-solid solution.

Conclusions

The divergent coordinate grid was used to determine the element distribution within the volume of the pentahedral prism by constructing a concentration stencil.

Using the eutectic reaction rule, eutectic temperatures were calculated, and the phase composition of interacting eutectics in the Fe – B – Mn – C – Cr system was determined.

To analyze the structural formation mechanisms during boriding in the liquid, crystallizing, or solid states of treated surfaces, it is recommended to use the constructed liquidus surface of the five-component phase diagram scheme for the Fe – B – Mn – C – Cr system, along with the calculated eutectic melting temperatures, which define the solidus surface of the system.

References / Список литературы

1. Lakhtin Yu.M., Leont'eva V.P. Materials Science. Moscow: Mashinostroenie; 1990:528. (In Russ.).
   Лахтин Ю.М., Леонтьева В.П. Материаловедение: Учебник для вузов. Москва: Машиностроение; 1990:528.
2. Zakharov A.M. Phase Diagrams of Binary and Ternary Systems. Moscow: Metallurgiya; 1990:240. (In Russ.).
   Захаров А.М. Диаграммы состояния двойных и тройных систем: Учебное пособие для вузов. Москва: Металлургия; 1990:240.
3. Campbell F.C. Phase Diagrams – Understanding the Basics. Materials Park, Ohio: ASM International; 2012:470.

4. Vozdvizhenskii V.M. Prediction of Binary State Diagrams. Moscow: Metallurgiya; 1975:224. (In Russ.).

Воздвиженский В.М. Прогноз двойных диаграмм состояния. Москва: Металлургия; 1975:224.

5. Massalski T.B. Binary Alloy. Phase Diagrams. 2nd ed. Vol. 3. ASM International; 1990:525.

6. Baker H. Introduction to Alloy Phase Diagrams: ASM Handbook. Vol. 3. ASM International; 1992:490.

7. Busby P.E., Warga M.E., Wells C. Diffusion and solubility of boron in iron and steel. *JOM*. 1953;(5):1463–1468. https://doi.org/10.1007/BF03397637

8. Carroll K.G., Darken L.S., Filer E.W., Zwell L. A new iron borocarbide. *Nature*. 1954;174:978–979. https://doi.org/10.1038/174978a0

9. Grange R.A. Boron, Calcium, Columbium, and Zirconium in Iron and Steel. New York: Wiley; London: Chapman and Hall; 1957:533.

Бор, кальций, ниобий и цирконий в чугуне и стали / Пер. с англ. В.А. Мчедлишвили и В.В. Ховрина; под ред. С.М. Винарова. Москва: Металлургиздат; 1961:459.

10. Voroshnin L.G., Lyakhovich L.S., Panich G.G., Protasevich G.F. Structure of alloys of the Fe-B system. *Metallovedenie i termicheskaya obrabotka metallov*.1970;(9):14–17. (In Russ.).

Ворошнин Л.Г., Ляхович Л.С., Панич Г.Г., Протасевич Г.Ф. Структура сплавов системы Fe–B. *Металловедение и термическая обработка металлов*. 1970;(9):14–17.

11. Koifman I.S., etc. X-ray analysis of boron cementite. *Metallovedenie i termicheskaya obrabotka metallov*.1969;(2):59–60. (In Russ.).

Койфман И.С. и др. Рентгенографический анализ борцементита. *Металловедение и термическая обработка металлов*. 1969;(2):59–60.

12. Stadelmaier H.H., Gregg R.A. Die Ternare Phase $Fe_{23}C_3B_3$ im Dreistoffsystem Eisen-Kohlenstoff-Bor. *Metall*. 1963; 17(5):412–414. (In Germ.)

13. Cameron T.B., Morral J.E. The solubility of carbon in iron. *Metallurgical Translations A*. 1986;17(8):1481–1483. https://doi.org/10.1007/bf02650132

14. Borlera Lucco M., Pradelli G. Iron-boron-carbon ratio system. *La Metallurgia Italiana*. 1967;59(11):907–916.

15. Samsonov G.V., Umanskii L.S. Solid Compounds of Refractory Metals. Moscow: Metallurgizdat; 1957:265. (In Russ.).

Самсонов Г.В., Уманский Л.С. Твердые соединения тугоплавких металлов. Москва: Металлургиздат; 1957:265.

16. Villars P., Prince A., Okamoto H. Handbook of Ternary Alloy Phase Diagrams. ASM International; 1994:1500.

17. Krukovich M.G., Prusakov B.A., Sizov I.G. Plasticity of Boronized Layers. Springer Series in Materials Science. Vol. 237. Springer International Publishing Switzerland; 2016:364. https://doi.org/10.1007/978-3-319-40012-9

18. Protsyuk A.P., Karapet'yants M.Kh. On the thermodynamic study of processes in multicomponent systems. *Zhurnal prikladnoi khimii*. 1977;50(1):169–171. (In Russ.).

Процюк А.П., Карапетьянц М.Х. О термодинамическом исследовании процессов в многокомпонентных системах. *Журнал прикладной химии*. 1977;50(1):169–171.

19. Gabdulin S.T., Baisanov S., Toleukadyr R.T. Constructing a phase diagram of the Fe – Mn – Si – C system to determine the phase composition of manganese ferroalloys. *Proceedings of the University: Karaganda State University*. Karaganda; 2020;(1(78)):38–43. (In Russ.).

Габдулин С.Т., Байсанов С., Толеукадыр Р.Т. Построение диаграммы состояния системы Fe – Mn – Si – C для определения фазового состава марганцевых ферросплавов. *Труды университета: Сборник трудов Карагандинского государственного университета*. Караганда; 2020;(1(78)):38–43.

20. Anosov V.Ya., Ozerova M.I., Fialkov Yu.Ya. Fundamentals of Physicochemical Analysis. Moscow: Nauka; 1976:503. (In Russ.).

Аносов В.Я., Озерова М.И., Фиалков Ю.Я. Основы физико-химического анализа. Москва: Наука; 1976:503.

21. Lodochnikov V.N. The simplest methods for representation multicomponent systems. *Izvestiya instituta fiziko-khimicheskogo analiza*. 1924;2(2):255–351. (In Russ.).

Лодочников В.Н. Простейшие методы изображения многокомпонентных систем. *Известия института физико-химического анализа*. 1924;2(2):255–351.

22. Radishchev V.P. Method for depicting multicomponent systems. *Izvestiya sektora fiziko-khimicheskogo analiza AN SSSR*. 1936;(9):203–219. (In Russ.).

Радищев В.П. Метод изображения многокомпонентных систем. *Известия сектора физико-химического анализа АН СССР*. 1936;(9):203–219.

23. Radishchev V.P. Methods for displaying multi-component diagrams. *Izvestiya sektora fiziko-khimicheskogo analiza AN SSSR*. 1938;(11):5–20. (In Russ.).

Радищев В.П. Методы изображения многокомпонентных диаграмм. *Известия сектора физико-химического анализа АН СССР*. 1938;(11):5–20.

24. Petrov D.A. State diagram of a five-component eutectic system in the coordinates of three-dimensional pentatopic projection. In: *State Diagrams of Metal Systems*. Moscow: Nauka; 1981:35–45. (In Russ.).

Петров Д.А. Диаграмма состояния пятикомпонентной эвтектической системы в координатах трехмерной проекции пентатопа. В кн.: *Диаграммы состояния металлических систем: Сборник трудов*. Москва: Наука; 1981: 35–45.

25. Ding M.X.U.K., Jow T. Phase diagram of EC-DMC binary system and enthalpic determination of its eutectic composition. *Journal of Thermal Analysis and Calorimetry*. 2000;61(1):177–186. https://doi.org/10.1023/A:1010175114578

26. Ramkumer K.L., Saxena M.K., Deb S.B. Experimental evaluation of procedures for heat capacity measurements by differential scanning calorimetry. *Journal of Thermal Analysis and Calorimetry*. 2001:66(2):387–397. https://doi.org/10.1023/A:1013126414406

27. Li S.-P., Zhao S.-X., Pan M.-X., Zhao D.-Q., Chen X.-C., Barabash O.M. Eutectic reaction and microstructural characteristics of Al(Li)–Mg2Si alloys. *Journal of Materials Science*. 2001;36(6):1569–1575. https://doi.org/10.1023/A:1017525520066

28. Lewis D., Allen S., Notis M., Scotch A. Determination of the eutectic structure in the Al–Cu–Sn system. *Journal of Electronic Material*. 2002;31(2):161–167. https://doi.org/10.1007/s11664-002-0163-y

29. Luo Ch.H., Martin M. Investigation of the phase diagram end the defect structure of non stoichiometric Li – Mn – O spiral. In: *Proceedings of the European Material Research Society Spring Meeting, May 24 – 28*. *Strasbourg*. 2004:28–32.

30. Krukovich M.G. Calculation of eutectic temperature and concentration in multicomponent systems. Moscow State University of Railway Engineering. Deposited in the All-Russian Institute of Scientific and Technical Information. Moscow; 1993;(3078-V95):10. (In Russ.).

Крукович М.Г. Расчет эвтектической температуры и концентрации в многокомпонентных системах. Московский государственный университет путей сообщения. Депонирована в Всероссийском институте научной и технической информации, 15.12.93, № 3078 – В95. Москва; 1993:10.

31. Krukovich M.G. Calculation of eutectic temperature and concentration in multicomponent systems. *Metallovedenie i termicheskaya obrabotka metallov*. 2005;(10):9–17. (In Russ.).

Крукович М.Г. Расчет эвтектических концентраций и температуры в двух- и многокомпонентных системах. *Металловедение и термическая обработка металлов*. 2005;(10):9–17.

32. Ganiev A.A., Khalikov A.R., Kabirov R.R. The development of calculation methods of concentrations and state diagram temperatures. *Mashinostroenie. Metallovedenie i termicheskaya obrabotka metallov. Vestnik Ufimskogo gosudarstvennogo aviatsionnogo universiteta*. 2008;11(2):116–122. (In Russ.).

Ганиев А.А., Халиков А.Р., Кабиров Р.Р. Разработка методики расчета эвтектических концентраций и температур диаграмм состояния. *Машиностроение. Металловедение и термическая обработка металлов. Вестник Уфимского государственного авиационного университета*. 2008;11(2):116–122.

33. Khalikov A.R. Modelling of eutectic concentrations of multicomponent constitution diagrams. *Mashinostroenie. Vestnik Ufimskogo gosudarstvennogo aviatsionnogo universiteta*. 2010;14(2):188–194. (In Russ.).

Халиков А.Р. Моделирование эвтектических концентраций многокомпонентных диаграмм состояния. *Машиностроение. Вестник Уфимского государственного авиационного университета*. 2010;14(2):188–194.

34. Egorova G.F., Afanas'eva O.S., Kaidalova L.V. Calculation of the composition and temperatures of peritectics of two-component systems using known melting temperatures. In: *Mathematical Modeling and Boundary Value Problems. Materials of the XI All-Russ. Sci. Conf. (May 27–30, 2019, Samara, Russian Federation). Vol. 1*. Samara: SamSTU; 2019:264–270. (In Russ.).

Егорова Г.Ф., Афанасьева О.С., Кайдалова Л.В. Расчет состава и температур перитектик двухкомпонентных систем по известным температурам плавления. В кн.: *Математическое моделирование и краевые задачи. Материалы XI Всероссийской научной конференции (27–30 мая 2019 г., Самара, РФ). Т. 1.* Самара: СамГТУ; 2019:264–270.

35. Amuda M.O.H, Akabekwa R.O. Estimating the eutectic composition of simple binary alloy system using linear geometry. *Leonardo Journal of Sciences*. 2008;12:232–242.

36. Krukovich M.G., Prusakov B.A., Sizov I.G. Plasticity of Boronized Layers. Moscow: FIZMATLIT; 2010:384. (In Russ.).

Крукович М.Г., Прусаков Б.А., Сизов И.Г. Пластичность борированных слоев. Москва: ФИЗМАТЛИТ; 2010:384.

37. Krukovich M.G. Technology to improve the performance properties of heterogeneous boronized layers. *Materials Performance and Characterization*. 2020;9(3):329–338. https://doi.org/10.1520/MPC20190091

38. Krukovich M.G., Baderko E.A., Kazakevich G.A. Modeling the patterns of growth of borated layers when heated by high-frequency current. In: *New Materials and Technologies in Mechanical Engineering: Proceedings*. 2023;38:41–45. (In Russ.).

Крукович М.Г., Бадерко Е.А., Казакевич Г.А. Моделирование закономерностей роста борированных слоев при нагреве ТВЧ. *Новые материалы и технологии в машиностроении: Сборник трудов*. 2023;38:41–45.

39. Pradelli G., Gianoglio C. Equilibri allo stato solido nel sistema cromo-manganese-boro. *La Metallurgia Italiana*. 1976;68(4):191–194. (In It.).

40. Krukovich M.G. Computation of eutectic concentrations and temperature in two-component and multicomponent systems. *Metal Science and Heat Treatment*. 2005;47:447–454. https://doi.org/10.1007/s11041-006-0009-y

Information about the Authors / Сведения об авторах

Grigorii A. Kazakevich, *Postgraduate of the Chair "Technology of Transport Engineering and Repair of Rolling Stock"*, Russian University of Transport
ORCID: 0009-0007-1542-979X
E-mail: KazakevichG@mail.ru

Aleksei Yu. Popov, *Cand. Sci. (Eng.), Assist. Prof. of the Chair "Technology of Transport Engineering and Repair of Rolling Stock"*, Russian University of Transport
ORCID: 0000-0002-3397-9484
E-mail: madrat@inbox.ru

Григорий Алексеевич Казакевич, *аспирант кафедры «Технология транспортного машиностроения и ремонта подвижного состава»*, Российский университет транспорта
ORCID: 0009-0007-1542-979X
E-mail: KazakevichG@mail.ru

Алексей Юрьевич Попов, *к.т.н., доцент кафедры «Технология транспортного машиностроения и ремонта подвижного состава»*, Российский университет транспорта
ORCID: 0000-0002-3397-9484
E-mail: madrat@inbox.ru

Received 09.07.2024
Revised 02.09.2024
Accepted 29.10.2024

Поступила в редакцию 09.07.2024
После доработки 02.09.2024
Принята к публикации 29.10.2024